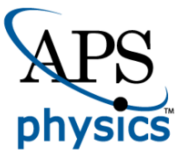

Transition to the Ultimate State of Turbulent Rayleigh-Bénard Convection

Xiaozhou He, Denis Funfschilling, Holger Nobach, Eberhard Bodenschatz, and Guenter Ahlers

Phys. Rev. Lett. **108**, 024502 — Published 9 January 2012

DOI: 10.1103/PhysRevLett.108.024502

Transition to the ultimate state of turbulent Rayleigh-Bénard convection

Xiaozhou He[1], Denis Funfschilling[2], Holger Nobach[1], Eberhard Bodenschatz[1,3,4], and Guenter Ahlers[5]
[1] *Max Planck Institute for Dynamics and Self Organization, D-37073 Göttingen, Germany*
[2] *LRGP CNRS - GROUPE ENSIC, BP 451, 54001 Nancy Cedex, France*
[3] *Institute for Nonlinear Dynamics, University of Göttingen, D-37073 Göttingen, Germany*
[4] *Laboratory of Atomic and Solid-State Physics and Sibley School of Mechanical and Aerospace Engineering, Cornell University, Ithaca, New York 14853*
[5] *Department of Physics, University of California, Santa Barbara, CA 93106, USA,*

Measurements of the Nusselt number Nu and of a Reynolds number Re_{eff} for Rayleigh-Bénard convection (RBC) over the Rayleigh-number range $10^{12} \lesssim \mathrm{Ra} \lesssim 10^{15}$ and for Prandtl numbers Pr near 0.8 are presented. The aspect ratio $\Gamma \equiv D/L$ of a cylindrical sample was 0.50. For $\mathrm{Ra} \lesssim 10^{13}$ the data yielded $\mathrm{Nu} \propto \mathrm{Ra}^{\gamma_{eff}}$ with $\gamma_{eff} \simeq 0.31$ and $\mathrm{Re}_{eff} \propto \mathrm{Ra}^{\zeta_{eff}}$ with $\zeta_{eff} \simeq 0.43$, consistent with classical turbulent RBC. After a transition region for $10^{13} \lesssim \mathrm{Ra} \lesssim 5 \times 10^{14}$, where multi-stability occurred, we found $\gamma_{eff} \simeq 0.38$ and $\zeta_{eff} = \zeta \simeq 0.50$, in agreement with the results of Grossmann and Lohse [1] for the large-Ra asymptotic state with turbulent boundary layers which was first predicted by Kraichnan [2].

In a fluid between horizontal parallel plates and heated from below, turbulent convection (known as Rayleigh-Bénard convection or RBC) occurs when the temperature difference $\Delta T = T_b - T_t$ between the bottom (T_b) and top (T_t) plates is sufficiently large [3, 4]. When a dimensionless measure of ΔT known as the Rayleigh number Ra exceeds a typical value $\mathrm{Ra}^* = \mathcal{O}(10^{14})$ [5, 6], the system is expected to undergo a transition. Below Ra^* the turbulent heat transport is limited by laminar boundary layers (BLs) below the top and above the bottom plate. Above Ra^* the shear applied to the BLs by the turbulent interior is expected to rendered the BLs turbulent as well [1, 2, 7], thus leading to a different heat-transport mechanism. The state above Ra^* is believed to be asymptotic in the sense that it will prevail as Ra diverges. For that reason it has been referred to as the "ultimate regime" [8, 9]; we shall call it the ultimate state (we shall refer to turbulent RBC below Ra^* as the "classical" state). Aside from the intrinsic interest in the physics of this system, an extrapolation of the properties from typical experimental ranges $\mathrm{Ra} \lesssim 10^{12}$ [3] to $\mathrm{Ra} \simeq 10^{20}$ and higher, which is relevant to geo/astrophysical systems, requires an understanding of the ultimate state.

Over a decade ago Chavanne *et al.* [8–10] measured the Nusselt number Nu(Ra) (the dimensionless effective thermal conductivity) up to $\mathrm{Ra} \simeq 10^{15}$ for a cylindrical sample of aspect ratio $\Gamma \equiv D/L = 0.50$ (D is the diameter and L the height) using fluid helium near its critical point at about 5 K and 2 bars. Their data reveal a transition in Nu(Ra) near $\mathrm{Ra} = 2 \times 10^{11}$ which they interpreted as the transition near Ra^*. However, their Ra at the transition was much lower than the expected $\mathrm{Ra}^* = \mathcal{O}(10^{14})$ [5]. For this and other reasons [11] it seems unlikely to us that their BLs underwent the transition to turbulence characteristic of the transition from the classical to the ultimate state. However, the authors of Refs. [9] and [12] have a different interpretation [13] and still claim to have observed the ultimate-state transition. Also about a decade ago, Niemela *et al.* [14–16] measured Nu(Ra) up to $\mathrm{Ra} \simeq 10^{17}$ in a nominally equivalent experiment, and found no transition. Numerous other low-temperature experiments were conducted for $\Gamma = 0.50$ [17–20], especially by Roche *et al.* [12]. Some showed a transition and others did not. For the reasons given [11] it seems unlikely to us (but, we are told [13], not to the authors of Refs. [9] and [12]) that the BL transition to turbulence associated with the ultimate state was involved in them.

Here we report measurements of Nu(Ra) and of a Reynolds number $\mathrm{Re}_{eff}(\mathrm{Ra})$ (to be defined explicitly below) at close to ambient (as opposed to cryogenic) temperatures. Both Nu and Re_{eff} revealed a transition over the same range of Ra; this range spanned more than a decade from $\mathrm{Ra}_1^* \simeq 10^{13}$ to $\mathrm{Ra}_2^* \simeq 5 \times 10^{14}$ [6]. For $\mathrm{Ra} \leq Ra_1^*$ we found $\mathrm{Nu} \propto \mathrm{Ra}^{\gamma_{eff}}$ with $\gamma_{eff} \simeq 0.31$ and $\mathrm{Re}_{eff} \propto \mathrm{Ra}^{\zeta_{eff}}$ with $\zeta_{eff} \simeq 0.43$, consistent with numerous measurements and with predictions for classical RBC below Ra^* (*cf.* [3]). For $\mathrm{Ra} > \mathrm{Ra}_2^*$ we found $\gamma_{eff} \simeq 0.38$ and $\zeta_{eff} = \zeta \simeq 0.50$, in agreement with predictions for the ultimate state [1]. For $\mathrm{Ra}_1^* < \mathrm{Ra} < \mathrm{Ra}_2^*$ Re_{eff} followed a non-monotonic and not always unique complex path. The observed transition range (as opposed to a characteristic value of Ra^*) is not surprising since the BLs and the shear applied to them by the turbulent bulk are known to be spatially inhomogeneous [21]. The location of this range along the Ra axis is roughly consistent with the expected values of Ra^* [5] for a shear instability of the BLs. The multi-stability revealed by Re_{eff} in the transition range suggests that the transition is discontinuous in the sense that, for instance, Re_{eff} on the branch below and the branch above the transition do not evolve continuously one into the other. Further evidence for a discontinuous transition comes from an extrapolation of

Re_{eff} in the ultimate state to smaller Ra, which meets the classical branch at $\mathrm{Ra} \simeq 4 \times 10^{12}$, *i.e.* well below the transition range between the two states. We believe that our measurements revealed the transition from classical RBC to the ultimate state, and that they show this transition to be discontinuous.

A large cylindrical sample of height $L = 2.24$ m and diameter $D = 1.12$ m known as the High-Pressure Convection Facility II (HPCF-II) was placed in an even larger pressure vessel known as the "Uboot of Göttingen" at the Max Planck Institute for Dynamics and Self Organization in Göttingen, Germany [22, 23]. The Uboot and HPCF-II were filled with the gas sulfur hexafluoride (SF_6) at pressures up to 19 bars. The HPCF-II was completely sealed, except for a 2.5 cm inner-diameter tube which passed through the sidewall at mid height and permitted the gas to enter the HPCF-II from the Uboot. One tube end was accurately flush with the inside of the wall and the other end terminated in a remotely operable valve. Once filled with the valve open, the desired temperatures of the top and bottom plates were established, and after equilibration for about 8 hours the valve was closed and all desired measurements were made.

The Prandtl number $\mathrm{Pr} \equiv \nu/\kappa$ (ν is the kinematic viscosity and κ the thermal diffusivity) was 0.79 (0.86) near $\mathrm{Ra} = 10^{12}$ (10^{15}). The measurements were made at several mean temperatures $T_m = (T_t + T_b)/2$ and at various pressures. The Rayleigh number is given by $\mathrm{Ra} = \alpha g \Delta T L^3/\kappa\nu$. Here the isobaric thermal expansion coefficient α, as well as κ and ν, were evaluated at T_m, and g is the acceleration of gravity.

There was a small effect of $T_m - T_U$ on Nu which is described in Supplementary Material submitted with this Letter, but the overall shape of Nu(Ra) was not influenced by $T_m - T_U$. The reduced Nusselt numbers $\mathrm{Nu}_{red} \equiv \mathrm{Nu}/\mathrm{Ra}^{0.312}$ obtained with $T_m - T_U \lesssim -3$K are shown as solid black circles in Fig. 1. For $\mathrm{Ra} < \mathrm{Ra}_1^* \simeq 10^{13}$ they are described well by a power law with $\gamma_{eff} = 0.312$. As can be seen in the figure, that power law agrees extremely well with data from [14–16] (stars, red online) for $10^9 \lesssim \mathrm{Ra} \lesssim 3 \times 10^{12}$, and with data from [9] (small open circles, blue online) for $10^9 \lesssim \mathrm{Ra} \lesssim 10^{11}$. It also agrees well with recent DNS results [24] (open circles with plusses and error bars, purple online). For $\mathrm{Ra} \gtrsim 10^{13}$ the slope of our $\mathrm{Nu}_{red}(\mathrm{Ra})$ in the logarithmic plot, corresponding to $\gamma_{eff} - 0.312$, gradually increased with increasing Ra and reached values corresponding to $\gamma_{eff} \simeq 0.38$ at $\mathrm{Ra} = \mathrm{Ra}_2^* \simeq 5 \times 10^{14}$. The value of γ_{eff} above Ra_2^* is consistent with the prediction for the ultimate state [1, 2, 7]. An extrapolation from the largest-Ra data of a power law with $\gamma_{eff} = 0.38$ (solid slanting line in Fig. 1a) yields an estimate for a transition point of $\mathrm{Ra}^* \simeq 1.4 \times 10^{14}$.

The data of Niemela et al. [14–16] also show a slight increase of Nu above the $\mathrm{Ra}^{0.312}$ dependence, starting at Ra just below 10^{13}. However, they do not seem to have the resolution to clearly reveal a transition. Indeed the original authors interpreted them in terms of a single power law with a classical exponent $\gamma_{eff} \simeq 0.32$ [16] up to the highest Ra of their experiment. The Chavanne *et al.* data [9] clearly show a transition near $Ra = 2 \times 10^{11}$, but its origin is still unknown to us. The DNS data [24] do not show any transition up to their largest $\mathrm{Ra} = 2 \times 10^{12}$.

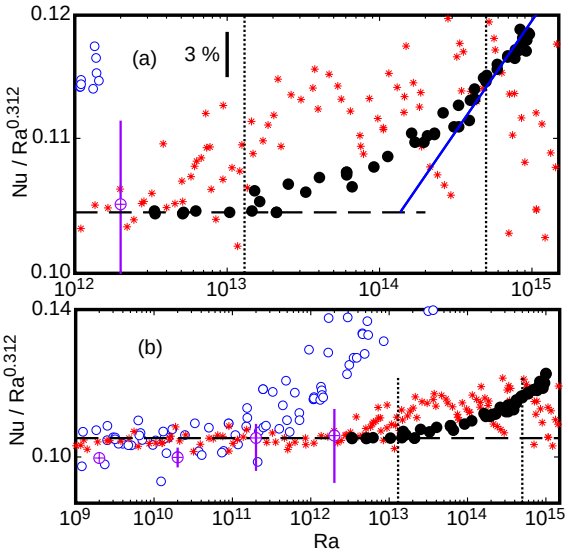

FIG. 1: $\mathrm{Nu}_{red} \equiv \mathrm{Nu}/\mathrm{Ra}^{0.312}$ as a function of Ra for the "closed" sample. Black solid circles: $T_m - T_U \lesssim -3$ K. Black open circles: $T_m - T_U \gtrsim +2$ K. Open squares (blue online): Nu_{red} of the open black circles multiplied by 1.04. Open diamonds (red online): Ra of the open squares divided by 3.7. Solid line (blue online) through the data at the largest Ra corresponds to $\gamma_{eff} = 0.38$. Vertical dotted lines: $\mathrm{Ra}_1^* = 1.3 \times 10^{13}$ and $\mathrm{Ra}_2^* = 5 \times 10^{14}$. Small stars (red online): Ref. [14]. Small open circles (blue online): Ref. [9]. Circles with plusses and error bars (purple online): DNS [24].

For the determinations of Re_{eff}, two thermistors were mounted, one above the other and separated by $r_0 = 3.0$ cm, at an average height $L/4$ above the bottom plate. The thermistors were placed about 1 cm from the side wall inside the sample. They were used to measure the local temperatures at a rate of 40 Hz, and it was assumed that temperature locally is a passive scalar so that its correlation function is the same as that of the velocity. The two time auto-correlation functions $C(0, \tau)$ and the cross-correlation function $C(r_0, \tau)$ were determined with high precision by averaging over time intervals of many hours for a given data point. The correlation functions were used to determine $V_{eff} = \sqrt{U^2 + V^2}$ and the corresponding $Re_{eff} = V_{eff} L/\nu$, using the elliptic approximation (EA). The EA was derived from a systematic second-order Taylor-series expansion of the space-time velocity correlation function [25, 26] and is well supported by experimental data [27–29]. The contribution U is the time-averaged vertical velocity component which turns out to be small compared to V, and V is the sum of v_0 [$v_0^2 = 2 \int E(k) dk$ and $E(k)$ is the energy spectrum of the

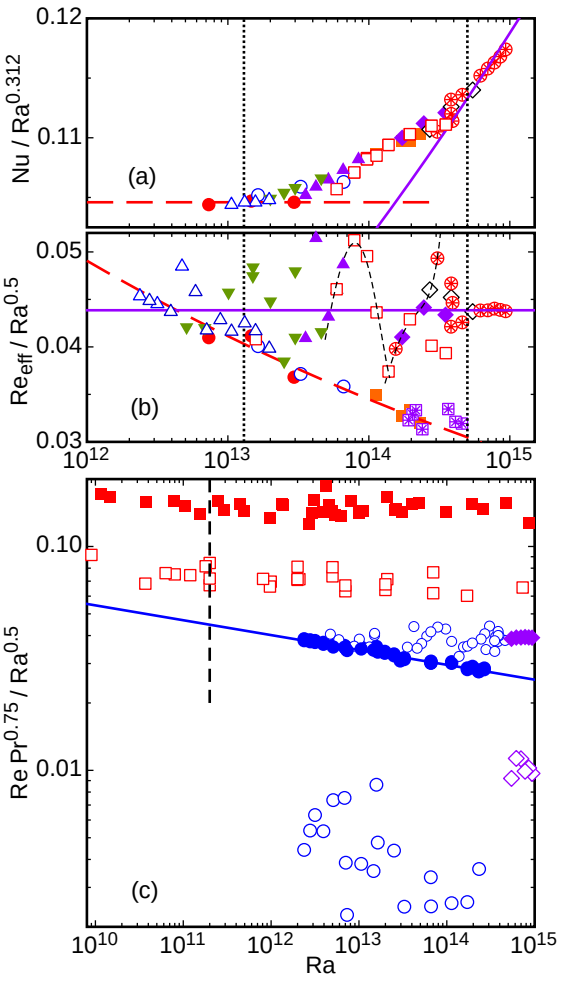

FIG. 2: a): $\mathrm{Nu}/\mathrm{Ra}^{0.312}$, b): $\mathrm{Re}_{eff}/\mathrm{Ra}^{0.5}$, and c): $\mathrm{RePr}^{0.75}/\mathrm{Ra}^{0.5}$, as a function of Ra. Different symbols in a) and b) correspond to different pressures and T_m and thus different Ra ranges. Squares with stars (purple online) in b): $T_m - T_U > 2K$; all others in a) and b): $T_m - T_U < -3\mathrm{K}$. Solid line (purple online) in a): $\mathrm{Nu} \sim \mathrm{Ra}^{0.38}$ and in b): $\mathrm{Re}_{eff} = 0.0439\mathrm{Ra}^{1/2}$. Dashed line (red online) in a): $\mathrm{Nu} = 0.105\mathrm{Ra}^{0.312}$ and in b): $\mathrm{Re}_{eff} = 0.407\mathrm{Ra}^{0.423}$. Black vertical dotted lines in a) and b): Ra_1^* and Ra_2^* as in Fig. 1. Vertical short dashed line in c): approximate location of the transition indicated by the data of [9] and shown in Fig. 1b. Thin short-dashed lines in (b) are guides to the eye and indicate the paths followed by the data. Solid squares (red online) in c): from [9]. Open squares (red online) in c): from [12]. Large solid (open) circles (blue online) in c): Re_{eff} ($\mathrm{Re}_U \equiv UL/\nu$) from this work, classical state. Small open circles in c): this work, transition region. Solid (open) diamonds (purple online) in c): Re_{eff} (Re_U) from this work, ultimate state. Solid line (blue online) in c): $\mathrm{Re}_{eff} = 0.252\mathrm{Ra}^{0.434}/\mathrm{Pr}^{0.750}$.

velocity] and of a very small contribution proportional to the local shear. A separate evaluation of U, V, and v_0 is possible as well (see, for instance, [27]).

In Fig. 2b we show results for $\mathrm{Re}_{eff}/\mathrm{Ra}^{1/2}$. The data fall into distinct groups. At relatively small $\mathrm{Ra} < \mathrm{Ra}_1^*$ they are described well by the long dashed line (red online), which corresponds to $\mathrm{Re}_{eff} = 0.407\mathrm{Ra}^{\zeta_{eff}}$ with $\zeta_{eff} = 0.423$. This classical state continues to exist up to $\mathrm{Ra}_2^* \simeq 5 \times 10^{14}$. For $\mathrm{Ra} \gtrsim \mathrm{Ra}_2^*$ the data are consistent with $\mathrm{Re}_{eff} = 0.0439\mathrm{Ra}^{\zeta}$ with $\zeta = 0.50$, which agrees with the prediction by Grossmann and Lohse [1] of a pure power law with $\zeta = 1/2$ for the ultimate state with turbulent BLs. A least-squares fit to the six points above Ra_2^* yields $\zeta = 0.504 \pm 0.006$. A much wider Ra range in the ultimate state obviously would be desirable, but is not accessible with our facility.

In addition to the classical state, a complex Ra dependence of Re_{eff} is observed in the range $\mathrm{Ra}_1^* \leq \mathrm{Ra} \leq \mathrm{Ra}_2^*$. Near and just above Ra_1^* the data seem to scatter randomly. For slightly larger Ra $\gtrsim 5 \times 10^{13}$ they fall on well defined, albeit non-monotonic, curves as indicated by the black short-dashed lines in Fig. 2b. The different symbols show that the results obtained at several different sample pressures, and thus different values of ΔT, reproduced this complex Ra dependence. There are also some points that do not fall on the short-dashed lines, suggesting multi-stability.

In Fig. 2a we show the results for Nu obtained simultaneously with the Re_{eff} measurements, with data taken at different pressures and T_m indicated by the same symbols as those used in Fig. 2b (note that these points are not the same as those shown in Fig. 1). Here one sees clearly that the Ra range of the transition region of Nu coincides with that of Re_{eff}. One also can see that the Nu results contain some of the complex dependences of $\mathrm{Re}_{eff}(\mathrm{Ra})$; but these complex effects are much less noticeable.

Finally, in Fig. 2c we collected our results for Re_{eff}, normalized by $\mathrm{Pr}^{0.75}$ and reduced by $\mathrm{Ra}^{0.5}$, in the classical (solid circles) and the ultimate (solid diamonds) states, as well as in the transition region (small open circles). The solid line through the classical data corresponds to $\mathrm{Re}_{eff} = 0.252\mathrm{Ra}^{\zeta_{eff}}/\mathrm{Pr}^{0.750}$ with $\zeta_{eff} = 0.434 \pm 0.003$, quite close to $\zeta_{eff} = 0.443$ obtained from the GL model for $\Gamma = 1$ [30]. Using the prediction $\mathrm{Re}_s = 0.48\sqrt{\mathrm{Re}_{eff}}$ [5], our result yields $\mathrm{Re}_s = 0.24\mathrm{Ra}^{0.217}/\mathrm{Pr}^{0.375}$ for the BL shear Reynolds number. For our Pr values this relationship gives $\mathrm{Re}_s = 183$, 300, and 398 for $\mathrm{Ra}_1^* = 1.3 \times 10^{13}$, $\mathrm{Ra}^* = 1.4 \times 10^{14}$, and $\mathrm{Ra}_2^* = 5 \times 10^{14}$ respectively. These values span the range of Re_s over which a BL shear instability would be expected. For the transition at $\mathrm{Ra} = 2 \times 10^{11}$ indicated by the data of Refs. [8, 9] one has $\mathrm{Re}_s \simeq 75$, which is too low for the BL shear instability.

Also shown in Fig. 2c are results from [12] (open squares, red online) and [9] (solid squares, red online). They are larger than ours. This is due to different measurement methods and definitions of Re. We note that the definition of Re_{eff} is unambiguous, based on properties of correlation functions, and given by the EA [as

explained above, to a good approximation it is equal to $\mathrm{Re}_{v_0} \equiv v_0 L/\nu$ with $v_0^2 = 2\int E(k)dk$]. Noteworthy is that the data of [12] and [9] show no change within their resolution of their Ra dependence at $\mathrm{Ra} \simeq 2 \times 10^{11}$ where the authors had observed a transition in their Nu measurements (see Fig. 1b) and where a change is expected if the transition is to the ultimate state. Our data show a clear discontinuity and a change of the dependence on Ra at the transition observed by us near $\mathrm{Ra} \simeq 5 \times 10^{14}$.

Further, we show in Fig. 2c the results for $\mathrm{Re}_U = UL/\nu$ based on the long-time average of the vertical velocity component U. We see that $\mathrm{Re}_U << \mathrm{Re}_{eff}$, and that Re_U and Re_{eff} both reveal a transition at the same value of Ra. We do not show $\mathrm{Re}_V \equiv VL/\nu = (\mathrm{Re}_{eff}^2 - \mathrm{Re}_U^2)^{1/2}$ because within the resolution of the figure it would be indistinguishable from Re_{eff}.

In this Letter we reported results for Nu(Ra) and Re_{eff}(Ra). For $\mathrm{Ra} \lesssim 10^{13}$ they are consistent with expectations for classical RBC [3, 5, 30]. For $\mathrm{Ra} \gtrsim 5 \times 10^{14}$ the Nu results agree with theoretical predictions for the ultimate state [1, 2, 7], but do not have the resolution to distinguish between the different predictions [1, 2] for the logarithmic corrections to a power law with exponent 1/2. In that large-Ra range the Re_{eff} results agree with the predictions of Grossmann and Lohse [1] of a pure power law with an exponent of 1/2 and no logarithmic corrections; they do not support the logarithms present in prior predictions [2]. At $\mathrm{Ra}_2^* = 5 \times 10^{14}$ both the fluctuation-dominated Re_{eff} and the mean-flow Re_U show a discontinuity, with a jump from the classical behavior at smaller Ra to the ultimate behavior at larger Ra. For the range $10^{13} \lesssim \mathrm{Ra} \lesssim 5 \times 10^{14}$ complex behavior associated with the transition from the classical to the ultimate state was observed for both Nu and Re. This transition range is consistent with a shear-induced transition to turbulent BLs, corresponding to a range of the shear Reynolds number from about 200 to 400. In view of the above evidence, we believe that we have found and characterized the transition to the ultimate (asymptotic) state of RBC.

Finally, we note that the ultimate-state exponents $\gamma_{eff} = 0.38$ and $\zeta = 0.50$ were found recently also for the corresponding variables in turbulent Taylor-Couette flow [31, 32]. There the BL shear is applied directly by the driving rather than indirectly by the induced LSC and fluctuations, and the classical turbulent state with laminar BLs and $\gamma_{eff} = 0.31$ and $\zeta_{eff} = 0.43$ has not yet been observed.

We are grateful to the Max-Planck Society and the Volkswagen Stiftung for their support. The work of G.A. was supported in part by the U.S National Science Foundation through Grant DMR07-02111. We are grateful to A. Kopp, A. Kubitzek, and A. Renner for their enthusiastic technical support. One of us (GA) appreciates helpful conversations with S. Grossmann and D. Lohse.

[1] S. Grossmann and D. Lohse, Phys. Fluids **23**, 045108 (2011).
[2] R. H. Kraichnan, Phys. Fluids **5**, 1374 (1962).
[3] G. Ahlers, S. Grossmann, and D. Lohse, Rev. Mod. Phys. **81**, 503 (2009).
[4] G. Ahlers, Physics **2**, 74 (2009).
[5] S. Grossmann and D. Lohse, Phys. Rev. E **66**, 016305 (2002).
[6] For certain other shear flows, such as pipe flow, it is well known that the transition to turbulence is not sharp and will depend on the prevailing perturbations of the laminar state. Thus we expect that Ra^* is only a typical value of Ra near which a transition may be seen rather than a sharp bifurcation point.
[7] E. A. Spiegel, Ann. Rev. Astron. Astrophys. **9**, 323 (1971).
[8] X. Chavanne, F. Chilla, B. Castaing, B. Hebral, B. Chabaud, and J. Chaussy, Phys. Rev. Lett. **79**, 3648 (1997).
[9] X. Chavanne, F. Chilla, B. Chabaud, B. Castaing, and B. Hebral, Phys. Fluids **13**, 1300 (2001).
[10] X. Chavanne, F. Chillá, B. Chabaud, B. Castaing, J. Chaussy, and B. Hébral, J. Low Temp. Phys. **104**, 109 (1996).
[11] Estimates of the boundary-layer (BL) shear Reynolds number Re_s [30] at the transition (based on our bulk Re_{eff} reported below) depend on Pr, but for Pr near one and $\mathrm{Ra} \simeq 2 \times 10^{11}$ are close to 70; the BL shear instability is not expected until $\mathrm{Re}_s \simeq 300$ to 400. Further, recent measurements and compilations of existing data [12] indicated that the observation of this transition is favored by larger Prandtl numbers Pr, whereas the BL shear instability is expected to be favored by smaller Pr. In addition, measurements of a bulk Re reported in Refs. [9] and [12] showed no change at the transition, whereas a significant change is expected [1, 2] and found in the present work near $\mathrm{Ra} = 5 \times 10^{14}$. Finally, DNS for Ra up to 2×10^{12} [24] has shown no transition.
[12] P.-E. Roche, F. Gauthier, R. Kaiser, and J. Salort, New J. Phys. **12**, 085014 (2010).
[13] P.-E. Roche, private communication, Nov. 2011.
[14] J. J. Niemela, L. Skrbek, K. R. Sreenivasan, and R. Donnelly, Nature **404**, 837 (2000).
[15] J. J. Niemela, L. Skrbek, K. R. Sreenivasan, and R. Donnelly, Nature **406**, 439 (erratum) (2000).
[16] J. J. Niemela and K. R. Sreenivasan, J. Low Temp. Phys. **143**, 163 (2006).
[17] P. E. Roche, B. Castaing, B. Chabaud, and B. Hebral, Phys. Rev. E **63**, 045303(R) (2001).
[18] P. Roche, F. Gauthier, B. Chabaud, and B. Hébral, Phys. Fluids **17**, 115107 (2005).
[19] F. Gauthier and P. Roche, EPL **83**, 24005 (2008).
[20] F. Gauthier, J. Salort, O. Bourgeois, J. Garden, R. du Puits, A. Thess, and P. Roche, EPL **87**, 44006 (2009).
[21] S. L. Lui and K.-Q. Xia, Phys. Rev. E **57**, 5494 (1998).
[22] G. Ahlers, D. Funfschilling, and E. Bodenschatz, New J. Phys. **11**, 123001 (2009).
[23] G. Ahlers, D. Funfschilling, and E. Bodenschatz, New J. Phys. **13**, 049401 (2011).
[24] R. J. A. M. Stevens, D. Lohse, and R. Verzicco, J. Fluid Mech. **688**, 31-43 (2011).

[25] G. W, He and J. B. Zhang, Phys. Rev. E **73**, 055303 (2006).
[26] X. Zhao and G.-W. He, Phys. Rev. E **79**, 046316 (2009).
[27] X. He, G. He, and P. Tong, Phys. Rev. E **81**, 065303 (2010).
[28] X. He and P. Tong, Phys. Rev. E **83**, 037302 (2011).
[29] Q. Zhou, C.-M. Li, Z.-M. Lu, and Y.-L. Liu, J. Fluid Mech. **683**, 94 (2011).
[30] S. Grossmann and D. Lohse, Phys. Rev. Lett. **86**, 3316 (2001).
[31] D. P. M. van Gils, S. G. Huisman, G.-W. Bruggert, C. Sun, and D. Lohse, Phys. Rev. Lett. **106**, 024502 (2011).
[32] S. G. Huisman, D. P. M. van Gils, S. Grossmann, C. Sun, and D. Lohse, Phys. Rev. Lett. (in print).